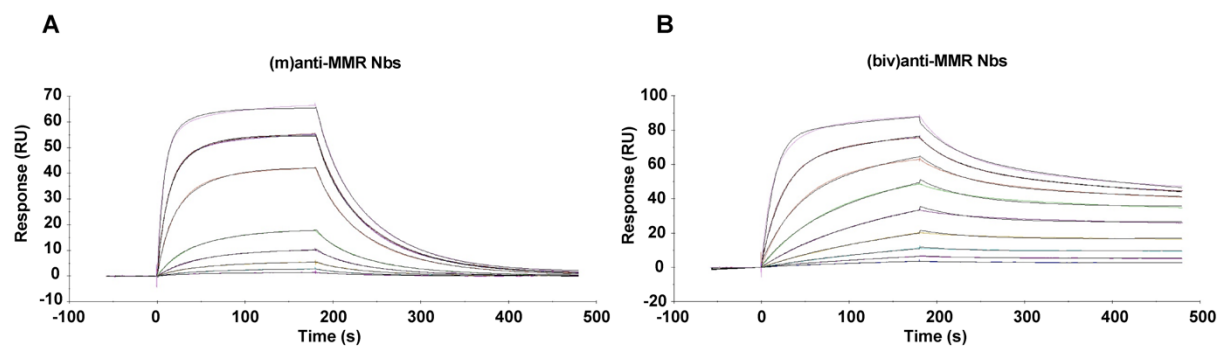


Supporting information:



	Ka1 (1/Ms)	Kd1 (1/s)	Ka2 (1/s)	Kd2 (1/s)	KD (M)	Chi ² (RU ²)
(m)anti-MMR Nb	9.820E+5	0.04196	0.01746	0.02463	2.500E-8	0.0607
(biv)anti-MMR Nb	8.563E+5	0.01680	0.006332	0.002158	4.987E-9	0.267
(dim)anti-MMR Nb	4.229E+5	0.03470	0.01196	0.02729	5.706E-8	0.0138

C

(m)anti-MMR Nb sequence with His tag

QVQLQESGGGLVQPGGSLRLSCAASGNIFSIAGWYRQAPGKQRELVATITLSGSTNYA
DSVKGRFSISRDNKNTVYLQMNSLKPEDTAVYYCNANTYSDSDVYGYWGQGTQVTVSSHHHHHH

(biv)anti-MMR Nb sequence with His tag

QVQLQESGGGLVQPGGSLRLSCAASGNIFSIAGWYRQAPGKQRELVATITLSGSTNYA
DSVKGRFSISRDNKNTVYLQMNSLKPEDTAVYYCNANTYSDSDVYGYWGQGTQVTVSSG
GGGSGGGSGGGGSQVQLQESGGGLVQPGGSLRLSCAASGNIFSIAGWYRQAPGKQRE
LVATITLSGSTNYADSVKGRFSISRDNKNTVYLQMNSLKPEDTAVYYCNANTYSDSDVY
GYWGQGTQVTVSSHHHHHH

(dim)anti-MMR Nb sequence with His tag

QVQLQESGGGLVQPGGSLRLSCAASGNIFSIAGWYRQAPGKQRELVATITLSGSTNYADSVKGRFSISRDNKNTVYL
QMNSLKPEDTAVYYCNANTYSDSDVYGYWGQGTQVTVSSAHHSEDPSSKAPKAPMAQVQLVESGGGSV
QA GGSRLSCTASGGSEYSYTFSLGWFRQAPGQEREAVAAIASMGGLTYASVKGRFTISRDNKNTVTL
QMNNLKPEDTAIYYCAVRGYFMRLPSSHNFRYWGQGTQVTVSSHHHHHH

D

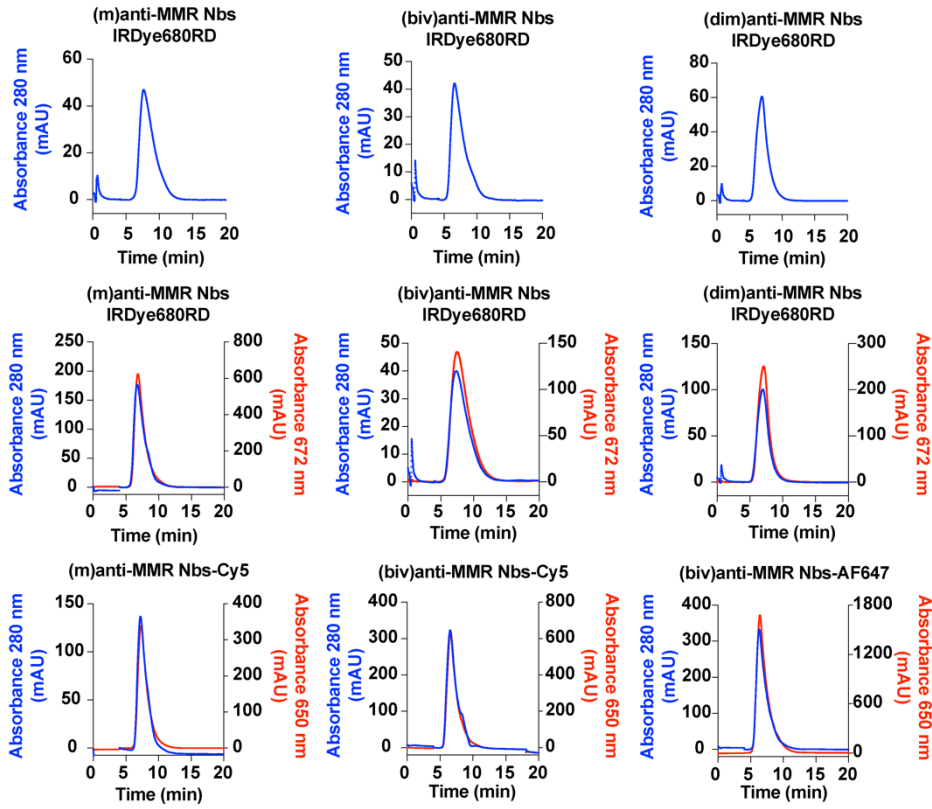
Molecular Weight of different (m), (biv) and (dim) constructs

	MMRCII (monovalent)	MMRCII-MMRCII (bivalent)	MMRCII-BCH10 (dimeric)
No Tag	12801 Da	28354 Da	26529 Da
6His tag	13625 Da	29178 Da	27353 Da
Cys	15059 Da	30612 Da	28787 Da

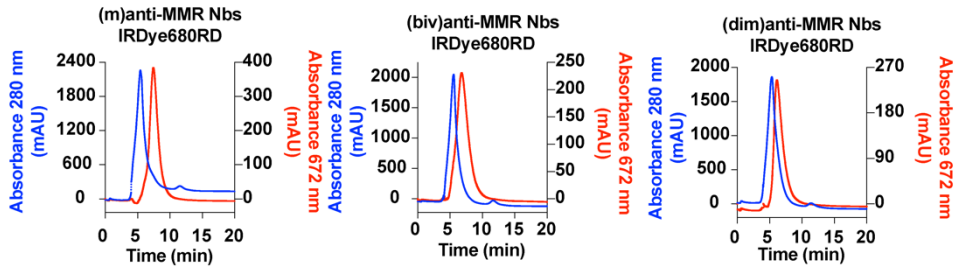
Supplementary Figure 1. Sequence and binding kinetics of the (m)anti-MMR Nb, (biv)anti-MMR Nb and (dim)MMR Nb on recombinant mouse MMR protein. (A) Association and

dissociation kinetic profiles of anti-MMR monovalent and bivalent Nbs as determined *via* surface plasmon resonance (SPR). (B) Calculated binding kinetic parameters k_a : association rate, k_d : dissociation rate, K_D : dissociation constant for (m)anti-MMR Nb, (biv)anti-MMR Nb and (dim)MMR Nb. C) Amino acid sequence coding for the (m)anti-MMR Nb, (biv)anti-MMR Nb and (dim)anti-MMR Nb containing a C-terminal hexahistidine tag. D) Molecular weight of different (m), (biv) and (dim) constructs.

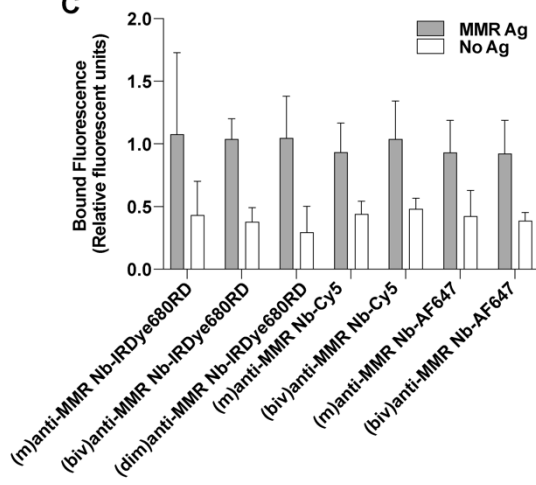
A



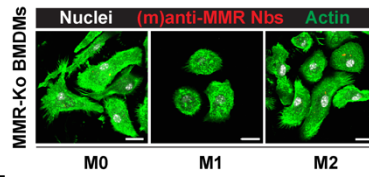
B



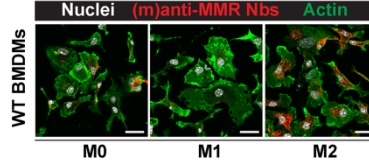
C



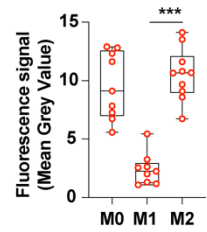
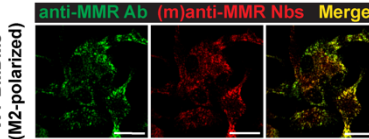
D



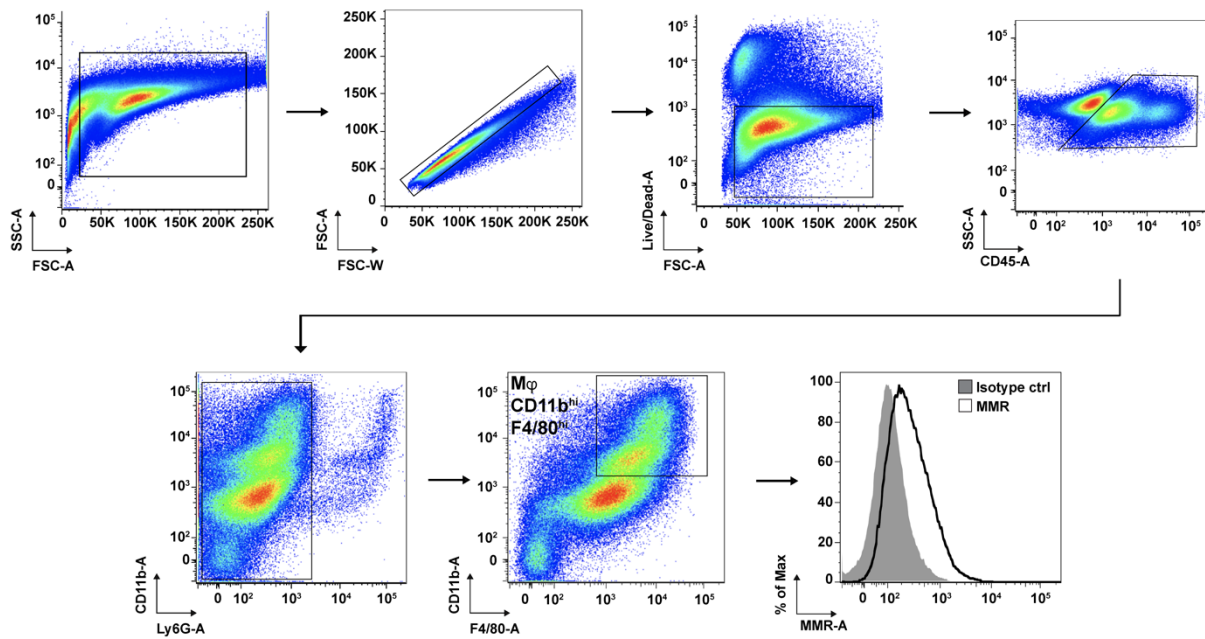
E



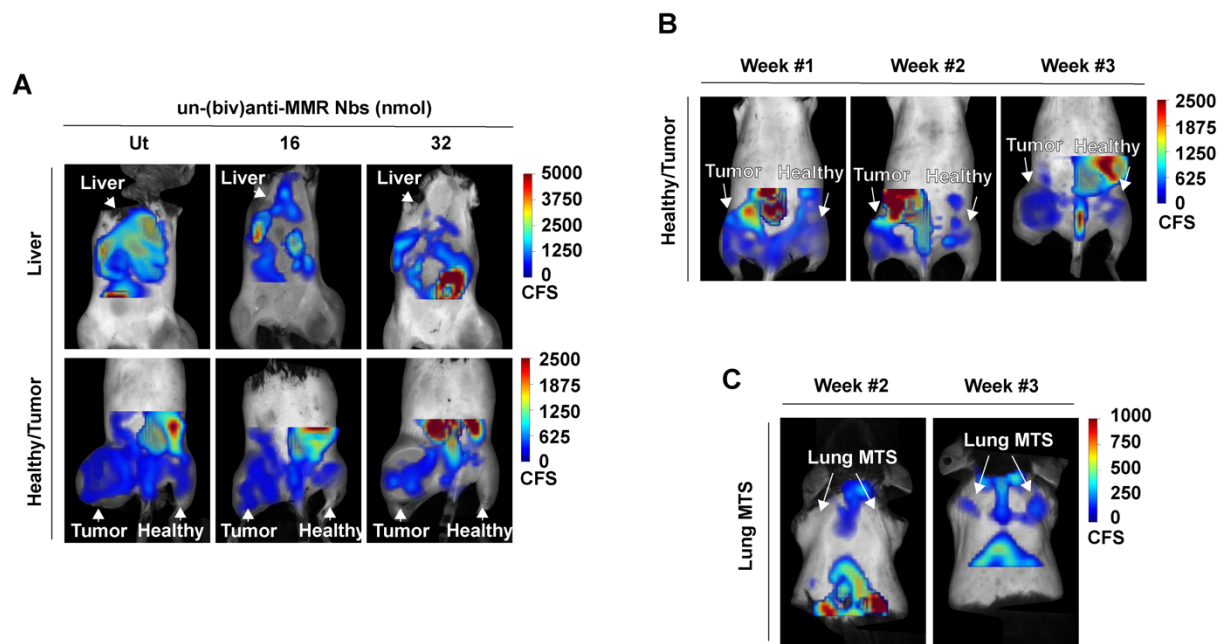
F



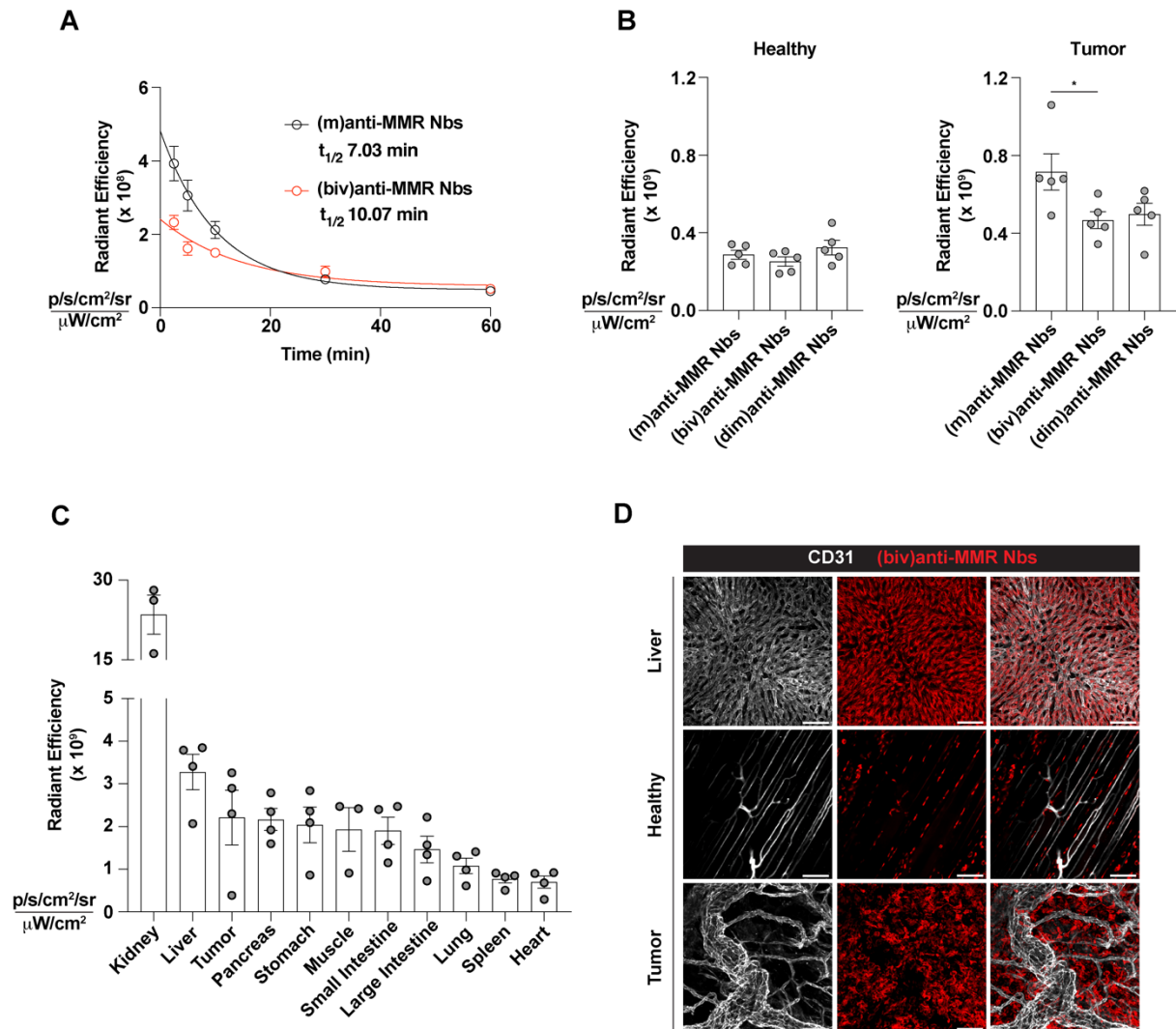
Supplementary Figure 2. Generation and validation of far-red and near infra-red dye-labelled anti-MMR Nbs. A) Validation of the purity of unlabelled, far-red and near infra-red dye-labelled anti-MMR Nbs by size exclusion chromatography. B) Demonstration of the *in vitro* stability of fluorescently labelled anti-MMR Nbs following incubation in serum for 3 h at 37 °C by size exclusion chromatography. C) Binding assay on recombinant MMR protein demonstrating the functionality of the fluorescently labelled MMR Nbs. D) Immunofluorescence confocal microscopy analysis of polarized bone marrow-derived macrophages, isolated from MMR-KO mice and incubated with Cy5-labelled (m)anti-MMR Nbs. Scale bar: 20 μ m. E) Immunofluorescence confocal microscopy analysis of polarized bone marrow-derived macrophages, isolated from WT mice and incubated with Cy5-labelled (m)anti-MMR Nbs. Scale bar: 20 μ m. Data are presented as box and whiskers plot (Min to Max). Every dot in the graph corresponds to a different image. Mann-Whitney test, *** $p < 0.001$. F) Immunofluorescence confocal microscopy analysis of M2-polarized macrophages, isolated from WT mice, incubated with Cy5-labelled (m)anti-MMR Nbs and co-stained with a monoclonal anti-MMR antibody revealed by AF488-labelled secondary antibody. Scale bar: 20 μ m.



Supplementary Figure 3. FACS analysis of MMR expression on tumor-associated macrophages. Gating strategy to evaluate the expression of MMR by tumor-infiltrating macrophages is shown.

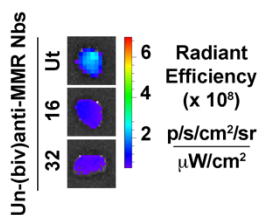
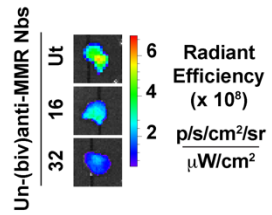
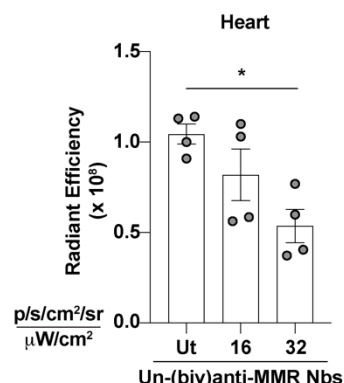
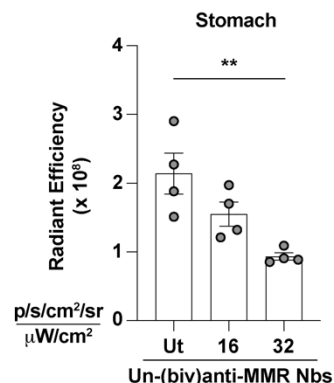
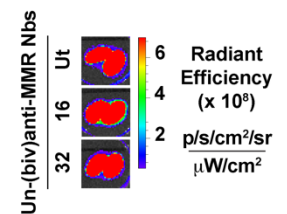
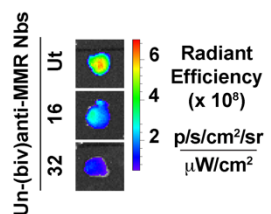
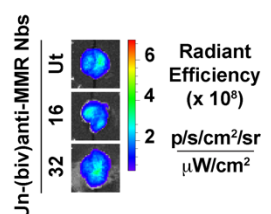
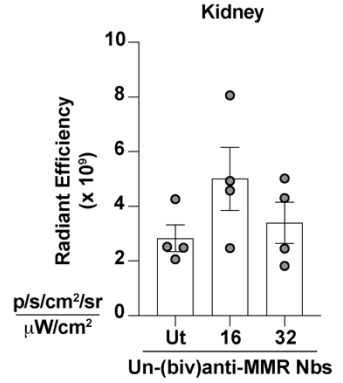
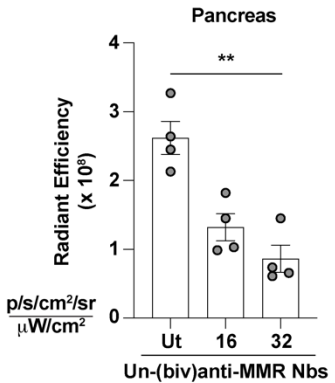
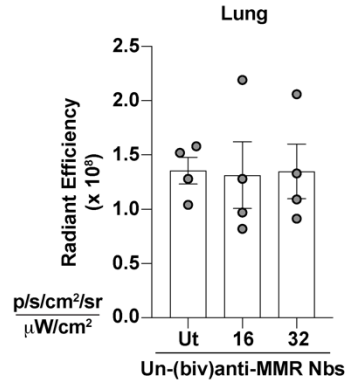
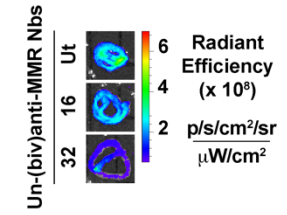
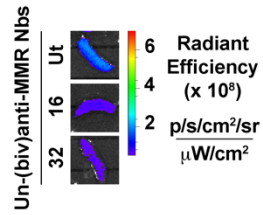
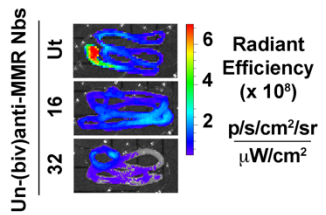
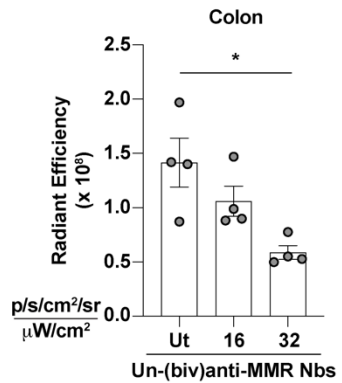
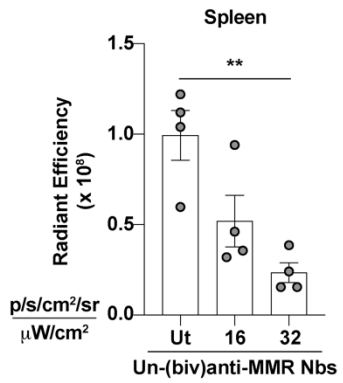
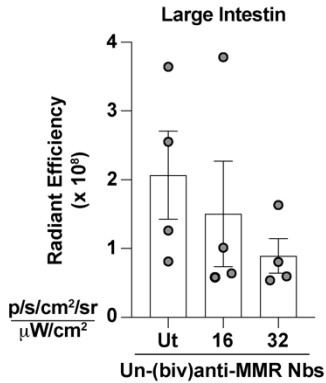


Supplementary Figure 4: Raw FMT fluorescence signal detected in tumor-bearing mice 1 hour after the injection of IRDye680RD-conjugated (m)anti-MMR Nbs. A) IRDye680RD-conjugated (m)anti-MMR Nbs accumulation in the abdominal cavity and tumor/healthy leg region, with or without the pre-administration of different doses of unlabelled (biv)anti-MMR Nbs. White arrows indicate the signal coming from the liver (upper panel) and primary tumor/corresponding healthy tissue (lower panel). CFS: Calibrated Fluorescence Signal. B) IRDye680RD-labeled (m)anti-MMR Nb accumulation in primary tumor/healthy leg region in 1-, 2- and 3-weeks tumor bearing mice. White arrows indicate the signal coming from the primary tumor/corresponding healthy tissue. CFS: Calibrated Fluorescence Signal. C) IRDye680RD-labeled (m)anti-MMR Nb accumulation in thoracic cavity in 2- and 3-weeks tumor bearing mice. White arrows indicate the occurrence of lung metastases 3 weeks after tumor cell injection. CFS: Calibrated Fluorescence Signal.



Supplementary Figure 5. A) Circulatory half-life of 2 nmoles of IRDye680RD-conjugated (m) and (biv)anti-MMR Nbs. Data are presented as Mean \pm SEM. One phase decay, $n=5$ B) Penetration of 2 nmoles of IRDye680RD-conjugated (m), (biv) and (dim)anti-MMR Nbs in tumor and corresponding healthy tissue. Every dot in the graph corresponds to an individual mouse. Data are presented as Mean \pm SEM. Kruskal-Wallis plus Dunn's Multiple comparison test, * $p<0.05$. C) *Ex vivo* biodistribution analysis of 32 nmoles of AF647-labelled (biv)anti-MMR Nb upon i.p. injection in 3 weeks tumor-bearing mice. Every dot in the graph corresponds to an individual mouse. Data are presented as Mean \pm SEM. D) Whole mount

confocal microscopy analysis of 32 nmoles of AF647-labelled (biv)anti-MMR Nb accumulation in liver, healthy muscle and tumor tissue, upon i.p. injection in 3 weeks tumor-bearing mice. Scale bar: 100 μ m.



Supplementary Figure 6. Biodistribution analysis of (m)anti-MMR Nbs upon the administration of a molar excess of unlabelled (biv)anti-MMR Nbs. Representative images of the acquired signal in the different organs are shown. Every dot in the graph corresponds to an individual mouse. Data are presented as Mean \pm SEM. Kruskal Wallis plus Dunn's Multiple comparison test, * $p < 0.05$, ** $p < 0.01$

Movie legends:

Movie1: Intravital microscopy of Cy5-labeled (m)anti-MMR Nbs in liver. Scale Bar: 100 μm .

Movie2: Intravital microscopy of Cy5-labeled (biv)anti-MMR Nbs in liver. Scale Bar: 100 μm .

Movie3: Intravital microscopy of Cy5-labeled (m)anti-MMR Nbs in liver upon the i.p. injection of 32nmol of un-(biv)anti-MMR Nbs. Scale bar: 100 μm .

Movie4: Intravital microscopy of Cy5-labeled (m)anti-MMR Nbs in healthy muscle tissue. Scale Bar: 100 μm .

Movie5: Intravital microscopy of Cy5-labeled (biv)anti-MMR Nbs in healthy muscle tissue. Scale Bar: 100 μm .

Movie6: Intravital microscopy of Cy5-labeled (m)anti-MMR Nbs in healthy muscle tissue upon the i.p. injection of 32nmol of un-(biv)anti-MMR Nbs. Scale bar: 100 μm .

Movie7: Intravital microscopy of Cy5-labeled (m)anti-MMR Nbs in tumor. Scale Bar: 100 μm .

Movie8: Intravital microscopy of Cy5-labeled (biv)anti-MMR Nbs in tumor. Scale Bar: 100 μm .

Movie9: Intravital microscopy of Cy5-labeled (m)anti-MMR Nbs in tumor upon the i.p. injection of 32nmol of un-(biv)anti-MMR Nbs. Scale bar: 100 μm .

Material and Methods:

Surface Plasmon Resonance (SPR)

SPR was performed using a Biacore device (Biacore T200; Cytiva). First, a CM5 sensor chip (Biacore, Series S Sensor Chip CM5; Cytiva) was activated with 1-ethyl-3-(3-dimethylaminopropyl)carbodiimide/N-hydroxysuccinimide (EDC/NHS; Amine Coupling Kit; Cytiva). Subsequently, recombinant murine MMR protein (2535-MM, R&D systems, 5 $\mu\text{g}/\text{mL}$) was immobilized on the chip at pH 5. The SPR measurements were done at 25 °C in HEPES buffered saline (HBS; Cytiva) as a running buffer, with a flow rate of 30 $\mu\text{L}/\text{min}$. For evaluation of the kinetic parameters (association rate k_a , dissociation rate k_d , dissociation constant K_D), the Nbs were injected consecutively in three-fold serial dilutions, from 100 to 0.4 nM. The association step was allowed for 180 s, the dissociation step for 600 s. Regeneration of 20 s at 30 $\mu\text{L}/\text{min}$ using 0.1 M glycine at pH 2.5 followed by a stabilization period of 60 s, was performed. The rate kinetic constants were determined by mathematical fitting using the 1:1 binding with drift and RI2 model proposed by the BIACORE Evaluation Software (Cytiva), and the k_d/k_a ratio was used to determine the equilibrium dissociation constant (K_D).

Macro (Fiji_ImageJ) to analyze the amount of Cy5-(m)anti-MMR Nbs within polarized macrophages.

```
run("Open...");  
imageTitle=getTitle();  
run("Set Measurements...", "area mean limit redirect=None decimal=2");  
run("Split Channels");  
selectWindow("C3-" + imageTitle);  
run("Close");
```

```

selectWindow("C1-" + imageTitle);
rename("Nbs");
selectWindow("C2-" + imageTitle);
run("Duplicate...", " ");
selectWindow("C2-" + imageTitle);
run("Median...", "radius=2");
setAutoThreshold("Default dark");
//run("Threshold...");
setThreshold(10, 255);
waitForUser("set the threshold and press OK, or cancel to exit macro");
setOption("BlackBackground", true);
run("Convert to Mask");
//run("Fill Holes");
run("Create Selection");
run("Set Measurements...", "area mean integrated limit redirect=[Nbs] decimal=2");
run("Measure");
waitForUser("save results, then press ok");
close("Threshold");
close("Results");
run("Close All");

```

Macro (Fiji_ImageJ) to analyse the Nb blood clearance in liver and healthy/tumor tissue

Liver:

```

run("Open...");
imageTitle=getTitle();
run("Split Channels");
selectWindow("C1-" + imageTitle);
rename("Dextran");
run("Duplicate...", "duplicate");

```

```

rename("Dextran_Duplicate");
selectWindow("C2-" + imageTitle);
rename("Nbs");
selectWindow("Dextran");
run("Threshold...");
waitForUser("Set threshold then press ok");
setOption("BlackBackground", true);
run("Convert to Mask", "method=Default background=Dark black");
getDimensions(width, height, channels, slices, frames);
p=frames;
for (n = 1; n <= p; n++) {
    Stack.setFrame(n);

run("Set Measurements...", "mean integrated limit display redirect=Nbs decimal=2");
run("Create Selection");
run("Make Inverse");
roiManager("Add");
run("Measure");
}
waitForUser("Check Analysis, Save Results, then press ok");
close("Threshold");
close("Results");
run("Close All");
close("ROI Manager");

```

Healthy/Tumor:

```

run("Open...");
imageTitle=getTitle();
run("Split Channels");
selectWindow("C2-" + imageTitle);

```

```
rename("Dextran");
run("Duplicate...", "duplicate");
rename("Dextran_Duplicate");
selectWindow("CI-" + imageTitle);
rename("Nbs");
selectWindow("Dextran");
run("Threshold...");
waitForUser("Set threshold then press ok");
setOption("BlackBackground", true);
run("Convert to Mask", "method=Default background=Dark black");
getDimensions(width, height, channels, slices, frames);
p=frames;
for (n = 1; n <= p; n++) {
    Stack.setFrame(n);

run("Set Measurements...", "mean integrated limit display redirect=Nbs decimal=2");
run("Create Selection");
//run("Make Inverse");
roiManager("Add");
run("Measure");
}
waitForUser("Check Analysis, Save Results, then press ok");
close("ROI Manager");
close("Results");
for (n = 1; n <= p; n++) {
    Stack.setFrame(n);

run("Set Measurements...", "mean integrated limit display redirect=Dextran_Duplicate decimal=2");
run("Create Selection");
//run("Make Inverse");
roiManager("Add");
```

```
run("Measure");  
}  
waitForUser("Check Analysis, Save Results, then press ok");  
close("Threshold");  
close("Results");  
run("Close All");  
close("ROI Manager");
```